Electronic Supplementary Material (ESI) for Journal of Materials Chemistry C.

Electronic Supplementary Information

Non-fullerene-based organic photodetectors for infrared communication

*Maxime Babics,[a] Helen Bristow,[b] Weimin Zhang,[c] Andrew Wadsworth,[b] Marios Neophytou,[c] Nicola Gasparini,[a] Iain McCulloch[bc]**

[a]Department of Chemistry and Centre for Plastic Electronics, Imperial College London, London, W12 0BZ, United Kingdom.
[b]Department of Chemistry, Chemistry Research Laboratory, University of Oxford, Oxford, OX1 3TA, United Kingdom.
[c]King Abdullah University of Science and Technology, KAUST Solar Center, Physical Sciences and Engineering Division (PSE), Thuwal, Saudi Arabia

**E-mail: iain.mcculloch@chem.ox.ac.uk*

S1. Synthetic protocol

Compound 2 To a solution of n-octylmagnesium bromide (1.0 M in THF, 50.0 mL, 50.0 mmol) was added lactone compound **1** (3.80 g, 9.79 mmol) at room temperature under argon, with stirring. The mixture was heated under reflux for 16 h. After cooled to room temperature, the reaction mixture was poured into ice water, followed by the extraction with ethyl acetate (3 × 100 mL). The combined extracts were washed with brine then dried over anhydrous Na_2SO_4. The solvent was removed under reduced pressure. The residue was dissolved in toluene (70 mL), then p-toluenesulfonic acid (1 g) was added. The mixture was stirred for 3 h then poured into water. The product was extracted with hexane (3 × 70 mL). The combined organic layers were dried over anhydrous Na_2SO_4. After removal of solvent, the residue was purified by column chromatography on silica, eluting with hexane, to give product as a yellow solid (5.78 g, 73%). ^{1}H NMR (500 MHz, $CDCl_3$) δ 7.00 (d, J = 5.2 Hz, 2H), 6.70 (d, J = 5.2 Hz, 2H), 1.92-2.14 (m, 8H), 1.54 – 1.17 (m, 48H), 0.86 (t, J = 6.9 Hz, 12H). ^{13}C NMR (126 MHz, $CDCl_3$) δ 151.61, 132.62, 129.00, 124.89, 120.92, 118.58, 110.50, 86.76, 39.02, 31.83, 29.90, 29.40, 29.23, 23.82, 22.65, 14.10. MALDI-TOF HRMS (m/z): $C_{48}H_{72}O_2S_4$ (M^+) calc. 808.4415, found 808.4422.

Compound 3 Compound **2** (3.22 g, 3.98 mmol) was dissolved in anhydrous chloroform (70 mL), followed by the addition of anhydrous DMF (3.0 g, 41.10 mmol) and $POCl_3$ (1.83 g, 11.92 mmol). This mixture was heated at reflux overnight (16 h), then poured into sodium acetate solution after cooled to room temperature. The resultant mixture was stirred for 3 h then extracted with DCM (3 ×70 mL). The extract was dried over Na_2SO_4. After removal of the solvent, the residue was purified by column chromatography with silica, eluting with hexane:DCM (2:1), to give product as a red solid (2.75 g, 80%). ^1H NMR (500 MHz, $CDCl_3$): δ 9.80 (s, 2H), 7.31 (s, 2H), 2.16 – 1.96 (m, 8H), 1.56 – 1.17 (m, 48H), 0.86 (t, $J = 6.9$ Hz, 12H); ^{13}C NMR (126 MHz, $CDCl_3$): δ 181.82, 152.04, 137.30, 134.86, 129.80, 128.98, 125.28, 121.35, 87.29, 39.30, 31.79, 29.74, 29.33, 29.17, 23.80, 22.63, 14.08. MALDI-TOF HRMS (m/z): $C_{50}H_{72}O_4S_4$ (M^+) calc. 864.4313, found 864.4317.

O4TIC To a solution of dialdehyde compound **3** (1.37 g, 1.58 mmol) and 2-(3-oxo-2,3-dihydro-1H-inden-1-ylidene)malononitrile (0.92 g, 4.74 mmol) in anhydrous chloroform (50 mL)was added pyridine (2 mL) dropwise under stirring at room temperature. This mixture was heated under reflux for 16 h. After cooled to room temperature, the solvent was removed under reduced pressure. The residue was purified by column chromatography on silica, eluting with DCM, to give product as a dark purple solid (1.12 g, 58%). ^1H NMR (500 MHz, CD_2Cl_2): δ 8.78 (s, 2H), 8.70 (d, $J = 7.8$ Hz, 2H), 7.93 (d, $J = 7.3$ Hz, 2H), 7.76-7.86 (m, 4H), 7.44 (s, 2H), 2.04-2.22 (m, 8H), 1.18-1.44 (m, 48H), 0.95-0.78 (m, 12H). MALDI-TOF HRMS (m/z): $C_{74}H_{80}N_4O_4S_4$ (M^+) calc. 1216.5062, found 1216.5070.

O4TFIC To a solution of dialdehyde compound **3** (1.05 g, 1.21 mmol) and 2-(5,6-difluoro-3-oxo-2,3-dihydro-1H-inden-1-ylidene)malononitrile (0.84 g, 3.65 mmol) in anhydrous chloroform (50 mL) was added pyridine (2 mL) dropwise under stirring at room temperature. This mixture was heated under reflux for 16 h. After cooled to room temperature, the solvent was removed under reduced pressure. The residue was purified by column chromatography on silica, eluting with DCM, to give product as a dark purple solid (0.96 g, 61%). ^1H NMR (500

MHz, CD_2Cl_2): δ 8.71 (s, 2H), 8.53 (dd, *J* = 10.1, 6.4 Hz, 2H), 7.66 (t, *J* = 7.6 Hz, 2H), 7.52 (s, 2H), 2.75 – 2.63 (m, 8H), 1.29-1.71 (m, 48H), 0.96 – 0.83 (m, 12H). ^{13}C NMR (126 MHz, CD_2Cl_2): δ 185.95, 152.64, 144.41, 140.23, 138.00, 136.68, 133.37, 132.84, 132.13, 131.95, 131.29, 128.48, 128.24, 122.15, 114.95, 114.29, 114.08, 112.50, 112.36, 88.01, 70.14, 35.58, 31.65, 31.24, 28.97, 22.58, 13.84. MALDI-TOF HRMS (m/z): $C_{74}H_{76}F_4N_4O_4S_4$ (M^+) calc. 1288.4686, found 1288.4692.

S2. General experiment details

PM6:O4TIC and PM6:O4TFIC organic photodetectors were fabricated on glass substrates with tin-doped indium oxide (ITO, 15 Ω sq^{-1}). Substrates are sonicated for 10 min each in successive baths of acetone and isopropanol. Next, the samples were dried with pressurized nitrogen before ozone plasma treatment for 10 min. A thin layer (~40 nm) of PEDOT:PSS was spin-cast onto the UV-treated substrates and dried on a heating plate at 140 °C for 20 minutes. The PEDOT-coated substrates were then transferred into a dry nitrogen glove box (< 3 ppm O_2).

The blend solutions were obtained by dissolving the PM6 purchased from one material and the NFAs in chlorobenzene (CB) using the donor-acceptor ratio of 1:1 (wt/wt), 30 mg/ml. The solutions were stirred overnight at 50 °C and were then cast on the PEDOT-coated substrates. The active layers were spin-cast from the hot solutions at 70 °C, at an optimized speed of 2000 rpm, for 45s, using a programmable spin coater; films were around 90 nm in thickness. For thermal annealing devices, samples were put on a hotplate at 130°C for 10 min. The Phen-DPO interlayer (0.5 mg/ml in isopropanol) was spincoated in the glovebox on top of the active layers at a speed of 2000 rpm for 20s. Next, the samples were placed in a thermal evaporator for deposition of a 100-nm thick silver electrode evaporated at 1 Å s^{-1} at a pressure under $2x10^{-6}$ Torr, through a shadow mask, giving an active layer area of 0.045 cm^2 per device.

JV response were performed using a Keysight source/monitor instrument.

Responsivity/EQE was measured by using a 100 W tungsten halogen lamp (Bentham IL1 with Bentham 605 stabilized current power supply) coupled to a monochromator with computer.

TPC and damping were performed using a Thorlab DC2200 LED driver mounted with a M880L3 LED (spectrum given in Figure S3). The M880L3 LED has a maximum irradiance of 5.6 μW mm^{-2} at a distance of 20 cm.

For the TPC the LED driver generates a repetitive square pulse of light of 200 μs followed by 200 μs of dark using LEDs with rise/decay times of less than 100 ns.

For the damping the LED driver generates a sinusoidal light at the desired frequency. The damping is measured according to the equation $dB_f = -20\log\left(\frac{I_f}{I_{fo}}\right)$ where I_f is the amplitude of the current at the light frequency f and $I_{f=0}$ is the amplitude of the current measured at constant illumination.

For both measurements the devices were placed 5 cm away from the IR LED. The photocurrent transients were obtained by measuring the voltage drop across a 50 Ω resistor using a Tektronix TDS3032B oscilloscope.

For the IV characteristic under light the devices were placed at distance of 2 cm from the light source.

The response signal from the commercial remote control (model F-TB-MINI-24, picture and spectrum given in Figure S3) the device was placed in dark 5 cm away from the commercial remote control. The photo response was acquired by measuring the voltage drop across a 50 Ω resistor with a Tektronix TDS3032B oscilloscope.

The capacitance of the OPDs with active layers of 90nm and pixel areas of 0.045cm^2 can be estimated assuming a dielectric constant of 3-4 according to the following equation.

$$C = \frac{\varepsilon_0 \varepsilon A}{d}$$

The resulting RC constant can be estimated as < 100 ns and the transient times determined for the OPDs can therefore be considered to be transport rather than RC limited.

S3. UV-vis absorption

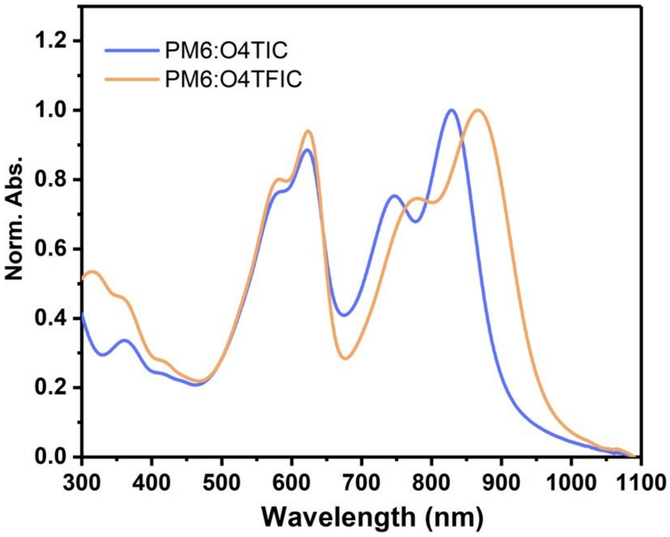

Figure S1. Thin-film UV-vis absorption spectra of PM6:O4TIC and PM6:O4TFIC

S4. PESA

Photoelectron spectroscopy in air (PESA) measurements were recorded using a Riken Keiki PESA spectrometer (Model AC-2) with a power setting of 10 nW and a power number of 0.3. Samples for PESA were prepared on glass substrates

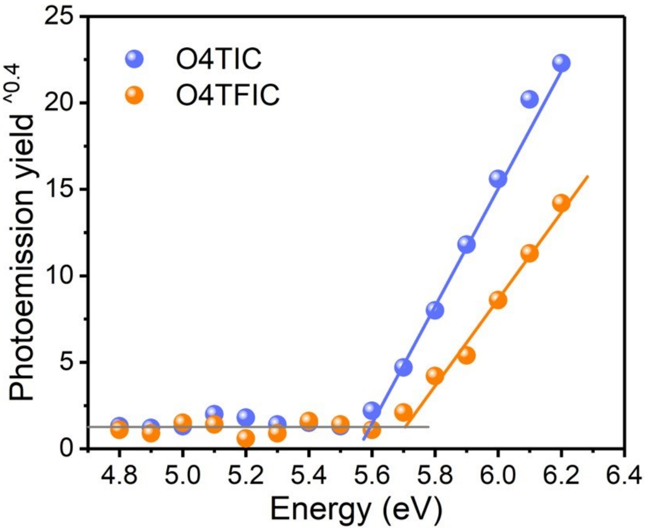

Figure S2. Superimposed PESA curves for O4TIC and O4TFIC.

S5 Emission LED

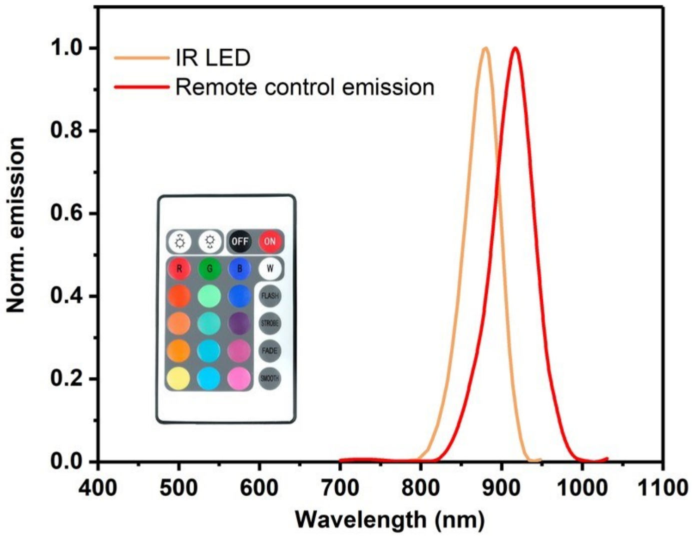

Figure S3. Superimposed spectrum of a commercial remote control and the IR LED used for light measurements.

S6. Thickness variation of PM6:O4TFIC

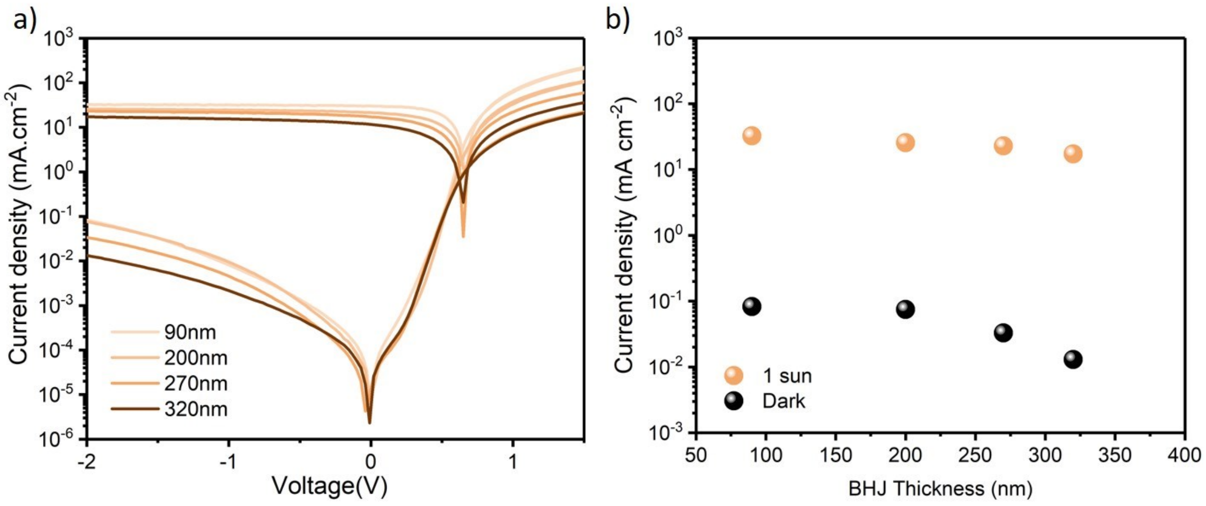

Figure S4. (a) Current-voltage measurement in dark and under one sun (AM1.5) for different thicknesses of PM6:O4TFIC BHJ (b) dark and one sun (AM1.5) current measured at -2V for different thicknesses of PM6:O4TFIC BHJ

Table S1. Summary of dark and light current (1 sun, AM1.5) measured at -2V for different thicknesses of PM6:O4TFIC BHJ.

Thickness (nm)	Dark current (μA.cm^2)
90	83
200	75
270	33
320	13

S7. Responsivity of a silicon solar cell

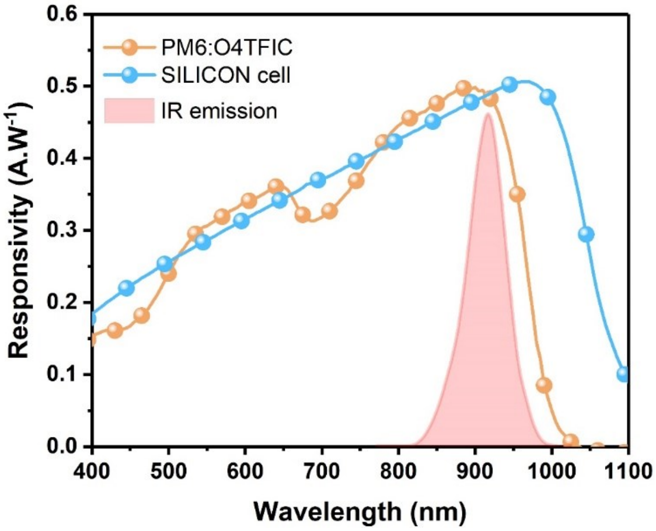

Figure S5. Superimposed responsivity of PM6:O4TFIC and a silicon detector.

S8. Noise current spectral density and specific detectivity

For the calculation of specific detectivity from the thermal, shot and flicker noise of the OPDs the following equation was used to determine the noise current (i_n). Where q is the elementary charge, i_d is the average dark current, k is the Boltzmann constant, T is the temperature, R_{shunt} is the shunt resistance, $i_{1/f}^2$ is the flicker noise obtained from the noise power spectral density and Δf is the bandwidth since flicker noise is frequency dependent.

$$(i_n)^2 = \left(2qi_d + \frac{4kT}{R_{shunt}} + i_{1/f}{}^2\right)\Delta f$$

Subsequently the specific detectivity was calculated from the following equation. Where A is the device area, Δf is the measurement bandwidth and R is the OPD responsivity.

$$D^* = \frac{\sqrt{A\Delta f}}{NEP} = \frac{\sqrt{A\Delta f}R}{i_n}$$

For the calculation of specific detectivity from the dark current density (J_d) the following equation is used. This method is widely used in literature but considered to give significant overestimations

$$D^* = \frac{R}{\sqrt{2qJ_d}}$$

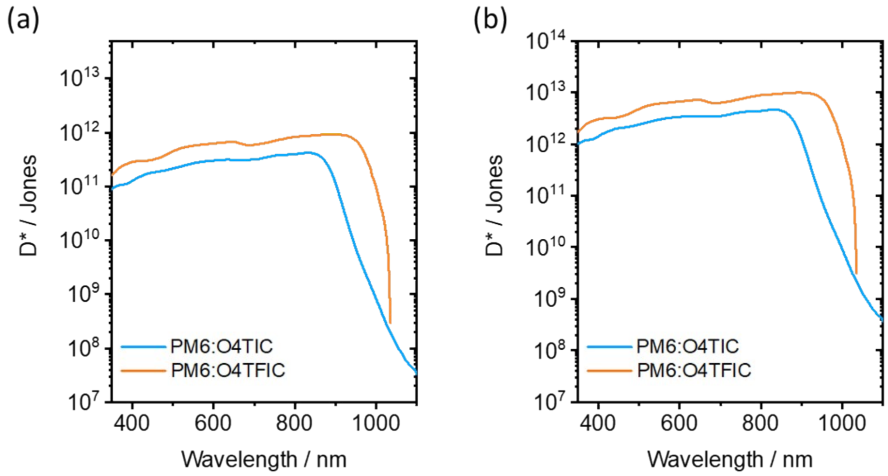

Figure S6. Specific Detectivity of PM6:O4TFIC and PM6:O4TIC based OPDs calculated from (a) Shot, Thermal and Flicker noise. (b) Dark current density.

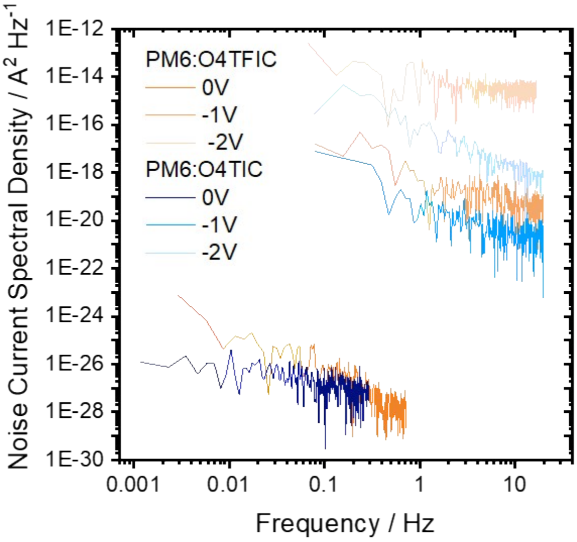

Figure S7. Noise spectral density determined by Fast Fourier Transform of the transient current at 0V, -1V and -2V for PM6:O4TIC, PM6:O4TFIC based OPDs.

S9. Transient photocurrent spectra (TPC)

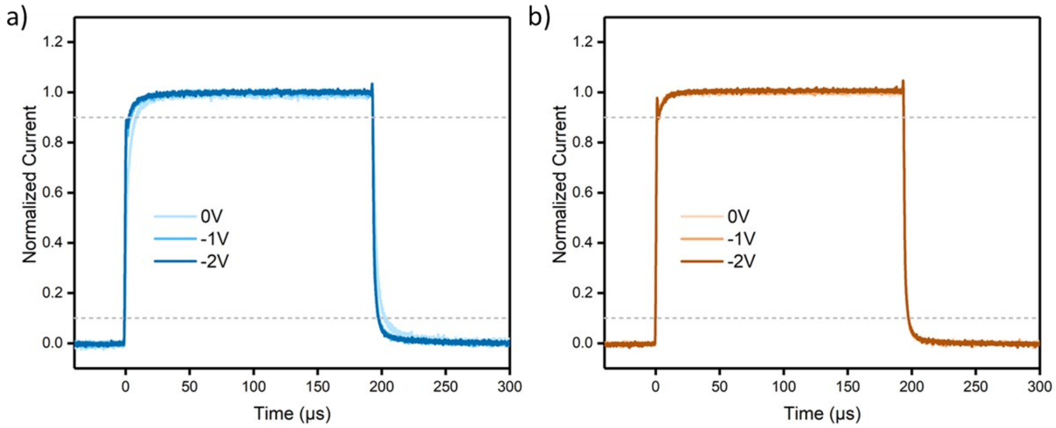

Figure S8. Transient current (normalized) for various voltage biases applied in response to 200 µs IR light pulse for (a) PM6:O4TIC and (b) PM6:O4TFIC. The transient time is the time taken to go from 10 % to 90 % of the steady state current.

Table S2. Summary of rise and decay times for PM6:O4TIC and PM6:O4TFIC for different applied voltage.

Voltage	PM6:O4TIC		PM6:O4TFIC	
	Rise time (μs)	Decay time (μs)	Rise time (μs)	Decay time (μs)
0	8.1	9.2	2.9	3.9
-1	4.8	4.7	2.8	3.6
-2	3.8	4.3	2.4	3.7

S10. SCLC mobilities

SCLC Measurements: The mobilities of the blends (electrons and holes) and neat materials were determined by fitting the dark current hole/electron-only diodes to the modified space-charge-limited current (SCLC) model. Hole-only diode configuration (Glass/ ITO/MoO3/BHJ/MoO3/Ag), V_{bi} = 0 V (flat band pattern formed by MoO3–MoO3). First, MoO3 (10 nm) was thermally evaporated onto the ITO-coated glass. After deposition of the active layer, using the same deposition conditions as discussed for organic solar cells above, MoO3 (7 nm) and Ag (100 nm) were deposited via thermal evaporation in a vacuum chamber through a shadow mask defining an active area of 0.045 cm^2. Electron-only diode configuration (Glass/ITO/ZnO/BHJ/Ca/ Al), V_{bi} = 1.5 V. The active layers were deposited on top of the ZnO/ITO-coated substrates. Ca (7 nm) and Al (100 nm) were deposited as the top electrode. The electric field–dependent SCLC mobility was estimated using the following equation derived from the theory of space-charge-limited current enhanced by Frenkel effect.[S1]

$$J(V) = \frac{9}{8}\varepsilon_0\varepsilon_r\mu_0 exp\left(0.89\beta\sqrt{\frac{V-V_{bi}}{L}}\right)\frac{(V-V_{bi})^2}{L^3}$$

Definition	Variable	Unit
Zero-field mobility	μ_0	cm^2 V^{-1} s^{-1}
Film thickness	L	cm
Dark current density	J	mA cm^{-2}
Voltage	V	V
Vacuum permittivity	$\varepsilon_0 = 88.54 \times 10^{-12}$	mA s V^{-1} cm^{-1}
Dielectric constant	$\varepsilon_r = 3$	
Field activation factor	β	cm$^{1/2}$ V$^{-1/2}$

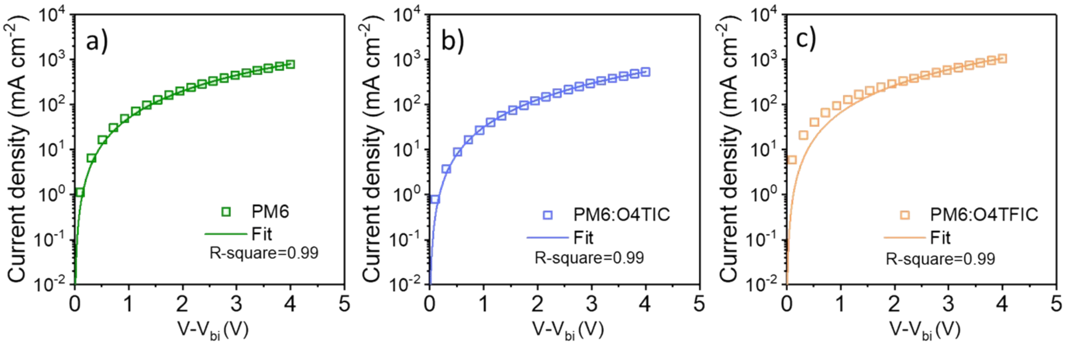

Figure S9: Hole only dark *J-V* curves of (a) neat PM6 (b) PM6:O4TIC and (c) PM6:O4TFIC devices. The solid lines are fits to the experimental data according to Equation 1.

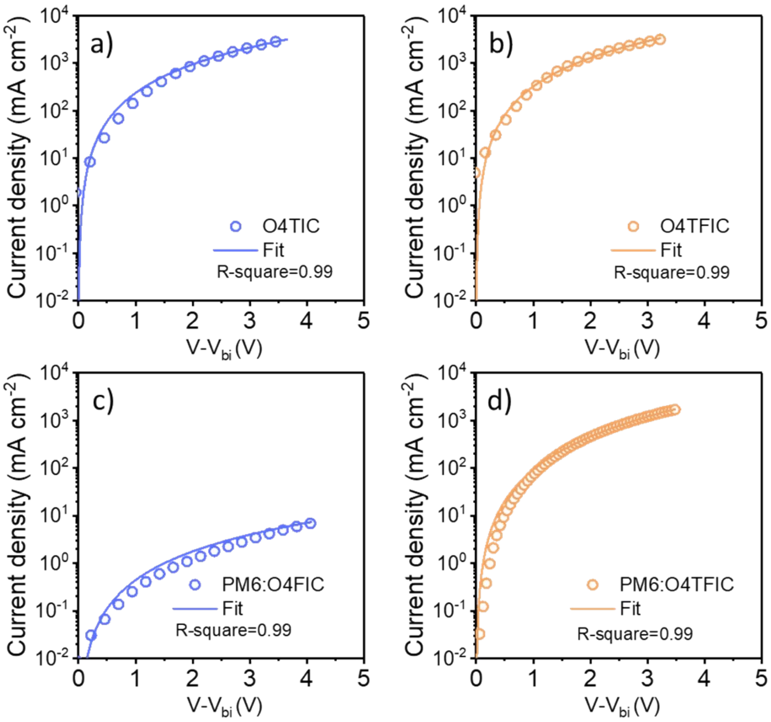

Figure S10: Electron only dark *J-V* curves of (a) neat O4TIC (b) O4TFIC and (c) PM6:O4TIC and (d) PM6:O4TFIC devices. The solid lines are fits to the experimental data according to Equation 1.

Table S3. Summary of SCLC mobilities for the neat films and the optimized blends

	μ_h (cm^2 V^{-1} s^{-1})	μ_e (cm^2 V^{-1} s^{-1})	$\mu_{h/}$ μ_e
PM6	1.7 ± 0.1 X 10^{-4}	-	-
O4TIC	-	1.4 ± 0.4 X 10^{-4}	-
O4TFIC	-	2.3 ± 0.1 X 10^{-4}	-
PM6:O4TIC	1.1± 0.1 X 10^{-4}	2.9 ± 1.1 X 10^{-6}	38
PM6:O4TFIC	2.5 ± 0.2 X 10^{-4}	1.3 ± 0.3 X 10^{-4}	2

[S1] Murgatroyd, P. N., Theory of space-charge-limited current enhanced by Frenkel effect. *J. Phys. D: Appl. Phys.* **1970,** *3* (2), 151.